

RESEARCH ARTICLE **OPEN ACCESS**

Vasopressin-Sensitive *Aqp2* Regulation Mediated by the TAZ-NR4A1 Axis in Renal Collecting Duct Cells

Hong Seok Choi^{1,2}  | Hyo-Ju Jang^{1,2}  | Wan-Young Kim³  | Sun Ah Park^{3,4}  | Euijung Park⁵  | Hyun Jun Jung⁶  | Tae-Hwan Kwon^{1,2} 

¹Department of Biochemistry and Cell Biology, Kyungpook National University, Taegu, Korea | ²BK21 FOUR KNU Convergence Educational Program, Department of Biomedical Science, School of Medicine, Kyungpook National University, Taegu, Korea | ³Department of Anatomy, Ajou University School of Medicine, Suwon, Korea | ⁴Department of Neurology, Ajou University School of Medicine, Suwon, Korea | ⁵Epithelial Systems Biology Laboratory, Systems Biology Center, National Heart, Lung, and Blood Institute, National Institutes of Health, Bethesda, Maryland, USA | ⁶Division of Nephrology, Department of Medicine, Johns Hopkins University School of Medicine, Baltimore, Maryland, USA

Correspondence: Hyun Jun Jung (hjung24@jhmi.edu) | Tae-Hwan Kwon (thkwon@knu.ac.kr)

Received: 5 March 2025 | **Revised:** 10 June 2025 | **Accepted:** 16 June 2025

Funding: This work was supported by grants from the National Research Foundation of Korea (NRF) grant funded by the Korea Government (MIST) (RS-2021-NR060094; RS-2023-NR077104). H.J.J. was financially supported by the Edward S. Kraus Scholar Award, Johns Hopkins University School of Medicine Division of Nephrology.

Keywords: aquaporin-2 | NR4A1 | renal collecting duct | TAZ | transcription factor | vasopressin

ABSTRACT

Regulation of aquaporin-2 (*Aqp2*) gene is essential for body water homeostasis. This study investigated how TAZ (a transcriptional coactivator with PDZ-binding motif, *Wwtr1*) controls vasopressin-driven AQP2 expression. AQP2 expression was studied using collecting duct-specific TAZ-knockout (TAZ^{fl/fl}; HoxB7Cre) mice and siRNA-mediated knockdown of TAZ in vasopressin-responsive mpkCCDc11 cells. Downstream factors of TAZ were identified using transcriptomics and bioinformatics. The TAZ^{fl/fl}; HoxB7Cre mice demonstrated polyuria and a significant decrease in AQP2 abundance in the kidney cortex and the outer medulla. dDAVP treatment (10⁻⁹ M, 24 h) on mpkCCDc11 cells significantly increased AQP2 mRNA and protein levels. However, siRNA-mediated TAZ knockdown (TAZ-KD) markedly attenuated these effects without affecting cAMP levels. Immunocytochemical analysis revealed a substantial decrease in AQP2 immunolabeling intensity in TAZ-KD cells following dDAVP stimulation. RNA sequencing analysis identified 1370 and 1985 differentially expressed genes in TAZ-KD cells under basal conditions and after dDAVP treatment, respectively. Among 17 previously identified transcription factor (TF) candidates, seven (*Nr4a1*, *Cebpb*, *Mef2d*, *Elf3*, *Klf5*, *Junb*, *Stat3*) were significantly upregulated by dDAVP in either control or TAZ-KD conditions. Among them, RT-qPCR analysis identified *Nr4a1* as a TAZ-dependent TF, and immunoblotting revealed reduced NR4A1 protein levels in TAZ-KD cells upon dDAVP stimulation. This finding suggests its role as a TAZ-regulated target in dDAVP response pathway. Accordingly, *Nr4a1*-KD reduced the dDAVP-induced upregulation of *Aqp2* mRNA and protein. KEGG pathway enrichment analysis revealed that HIF-1 signaling and glycolysis as central pathways affected by TAZ. TAZ-NR4A1 axis acts as a novel transcriptional regulatory mechanism in controlling vasopressin-mediated AQP2 expression.

Hong Seok Choi and Hyo-Ju Jang contributed equally to this study.

This is an open access article under the terms of the [Creative Commons Attribution-NonCommercial-NoDerivs](https://creativecommons.org/licenses/by-nc-nd/4.0/) License, which permits use and distribution in any medium, provided the original work is properly cited, the use is non-commercial and no modifications or adaptations are made.

© 2025 The Author(s). *The FASEB Journal* published by Wiley Periodicals LLC on behalf of Federation of American Societies for Experimental Biology.

1 | Introduction

The renal collecting duct is an important renal tubular segment responsible for regulating urine concentration and maintaining body water homeostasis [1, 2]. This physiological process is tightly regulated by arginine vasopressin, which increases water reabsorption in the collecting duct. Vasopressin achieves this by controlling both the expression and translocation of aquaporin-2 (AQP2), a water channel protein that facilitates osmotic water permeability across the apical plasma membrane of collecting duct principal cells [2–4]. The regulation of AQP2 in response to the activation of vasopressin signaling involves both short-term and long-term mechanisms [5, 6]. Vasopressin primarily increases the translocation of AQP2-containing vesicles and incorporation of AQP2 into the apical membrane of collecting duct principal cells through short-term regulation [7–10]. Long-term regulation, on the other hand, involves transcriptional activation of the *Aqp2* gene [6, 11, 12]. The vasopressin-mediated transcriptional regulation is highly selective; studies using RNA sequencing (RNA-Seq) and chromatin immunoprecipitation with sequencing (ChIP-Seq) have shown that only a small subset of genes, including *Aqp2*, are transcriptionally activated by vasopressin stimulation in mouse collecting duct cell models [12]. Transcriptional regulation of *Aqp2* involves various transcription factors (TFs), including GATA3, NFAT5, ELF3, and AP-1 [6, 11, 13–17]. These TFs interact with genomic regulatory elements within the *Aqp2* promoter region, including cAMP-responsive elements (CREs) and TPA response elements (TREs), to enhance transcription [11, 18]. For instance, ELF3 binds to an Ets element in the *Aqp2* promoter, thereby affecting vasopressin-inducible *Aqp2* gene expression levels [16]. Moreover, complex interactions between vasopressin signaling pathways, TFs, and epigenetic factors contribute to the transcriptional regulation of *Aqp2* [7, 19].

The Hippo signaling pathway regulates various cellular processes, including cell proliferation, cell differentiation, cell migration, and organ size regulation [20, 21]. Yes-associated protein (YAP) and the transcriptional coactivator with a PDZ-binding motif (TAZ), encoded by the *Wwtr1* gene, are key downstream effectors of this pathway that regulate gene expression through nuclear translocation [22]. Recent studies have implicated Hippo signaling components as part of the regulatory networks of *Aqp2* transcription. Specifically, YAP has been identified as a pivotal transcriptional coactivator for *Aqp2* in collecting duct cells, interacting with TFs such as GATA2, GATA3, and NFATc1 to enhance *Aqp2* expression [23]. The finding suggests a functional crosstalk between Hippo signaling components and vasopressin-mediated transcriptional networks. Moreover, TAZ has been demonstrated to play a critical role in cyst formation and growth in polycystic kidney disease (PKD), as part of the PKD1–TAZ–Wnt– β -catenin–c-MYC signaling axis [24].

TAZ (WW domain-containing transcription regulator protein 1: WWTR1), the paralog of YAP, shares considerable structural and functional similarities with YAP, and both proteins often exhibit redundant or compensatory roles as transcriptional coregulators [25, 26]. Additionally, *Yap1* and *Wwtr1* are expressed in kidney collecting ducts at the similar transcriptomic level (<https://esbl.nhlbi.nih.gov/MRECA/Nephron/>). It is therefore highly plausible that TAZ also participates in the regulatory network

governing *Aqp2* expression in collecting duct cells. While the role of YAP as a coactivator interacting directly with TFs to enhance *Aqp2* expression was demonstrated, the specific contribution of TAZ remains unexplored. Therefore, we hypothesize that TAZ may also regulate *Aqp2* expression by interacting with TFs. This study aimed to investigate whether vasopressin-induced AQP2 regulation is affected by TAZ, focusing on how TAZ affects TF expression levels for *Aqp2* expression in mouse cortical collecting duct cells. By exploring this potential regulatory axis, the study aimed to uncover novel mechanisms within the complex network governing vasopressin-driven AQP2 expression.

2 | Materials and Methods

2.1 | Cell Culture

Mouse kidney cortical collecting duct cells (mpkCCDc11 cells) were cultured in a 1:1 mixture of DMEM and Ham's F-12 medium (11330032, Thermo Fisher Scientific, Waltham, MA), containing 60 nM sodium selenite (S9133, Sigma, St. Louis, MO, USA), 5 μ g/mL transferrin (T8158, Sigma), 50 nM dexamethasone (D8893, Sigma), 1 nM triiodothyronine (T5516, Sigma), 10 ng/mL epidermal growth factor (E4127, Sigma), 5 μ g/mL insulin (I5500, Sigma), 1% antibiotic–antimycotic (15240062, Thermo Fisher Scientific), and 2% decomplemented fetal bovine serum (FBS, SV30207.02, Hyclone, Cytiva, Marlborough, MA, USA) at 37°C in the presence of 5% CO₂. To assess the response of cells to 1-deamino-8-D-arginine vasopressin (dDAVP, V1005, Sigma), cells were grown on semipermeable filters of the Transwell system (0.4 μ m pore size, Transwell Permeable Supports, 3450, Corning, NY, USA) in culture medium and in serum- and hormone-free medium for an additional 24 h before dDAVP treatment. dDAVP (10^{−9} M) was applied to the basolateral side of the cells for 24 h to induce a response. The passage number of the mpkCCDc11 cells used in this study ranged from 11 to 16.

2.2 | Collecting Duct-Specific TAZ-Knockout Mice

Experiments involving the collecting duct-specific TAZ-knockout (TAZ^{fl/fl}; HoxB7Cre) mice were conducted at the Catholic University of Korea, Seoul. The knockout mice were generated by crossing TAZ-floxed mice with HoxB7Cre transgenic mice. The TAZ-floxed mice, carrying TAZ alleles where exon 3 is flanked by loxP sites, were originally established at the Korea Advanced Institute of Science and Technology (KAIST) and were provided by Dae-Sik Lim [24, 27, 28]. The HoxB7Cre transgenic mice, which drive Cre-recombinase expression specifically in the renal collecting duct, were used, as previously described [24]. All mice were maintained on a C57BL/6 genetic background. They were housed in the animal facility under controlled conditions (12-h light/dark cycle, 20°C). All animal procedures were approved by the Animal Care and Use Committee at the Catholic University of Korea, Seoul (Approval Number: 17-004).

2.3 | Semiquantitative Immunoblotting

Mice were anesthetized under enflurane inhalation and right kidneys were rapidly removed. The right kidney was dissected

to cortex (COR), outer medulla (OM), and inner medulla (IM) and tissues were homogenized in boiling lysis buffer 1.0% sodium dodecyl sulfate (SDS), 1.0 mM sodium orthovanadate, and 10 mM Tris-Cl (pH 7.4) as previously described [29]. SDS-PAGE was performed on 12% polyacrylamide gels, as previously described [30]. Cells were washed with ice-cold PBS and lysed in Laemmli lysis buffer (10 mM Tris-HCl [pH 6.8] and 1.5% SDS) containing a protease and phosphatase inhibitor cocktail (Halt Protease and Phosphatase Inhibitor Cocktail 100×, 78440, Thermo Fisher Scientific). The lysates were collected with a cell scraper, placed in the QIAshredder column (79656, QIAGEN, Hilden, Germany), and centrifuged at 10000×g for 2 min at room temperature. Total protein concentration was measured using the Pierce BCA Protein Assay Kit (23227, Thermo Fisher Scientific). To obtain the nuclear and cytoplasmic protein extracts from mpkCCDc11 cells, NE-PER Nuclear and Cytoplasmic Extraction Reagents (78833, Thermo Fisher Scientific) were used according to the manufacturer's instructions, as we previously demonstrated [31]. To confirm whether nuclear and cytoplasmic extracts were properly separated, GAPDH and Lamin A/C were used as markers for cytoplasmic and nuclear fractions, respectively.

Semiquantitative immunoblotting was performed as previously described [32, 33]. The primary antibodies used were anti-AQP2 (1:1000, AB3274, Merck Millipore), anti-TAZ (1:1000, 560235, BD Biosciences, Franklin Lakes, NJ, USA), anti-phospho-TAZ (1:1000, #59971, Cell Signaling Technology, Danvers, MA, USA), anti-Nr4a1 (1:1000, ab153914, Abcam, Cambridge, UK), anti-GAPDH (1:3000, no. 2118, Cell Signaling Technology), anti-Lamin A/C (1:1000, no. 4777, Cell Signaling Technology), and anti-β-actin (1:200000, A1978, Sigma) antibodies. Proteins in immunoblots were detected using horseradish peroxidase-conjugated secondary antibodies (P447 or P448, Dako, Glostrup, Denmark). Band density was quantified using Image J (NIH, Bethesda, MD, USA). The loading control (β-actin) was assessed on a separate gel, run with identical samples and using the same loading volumes for immunoblotting [31]. The densitometry values for each protein were corrected by the densitometry value of β-actin [31].

2.4 | Small Interfering RNA (siRNA)-Mediated Protein Knockdown (KD)

To examine the effects of TAZ-KD or Nr4a1-KD on the dDAVP-induced changes in AQP2 expression, mpkCCDc11 cells transfected with control-siRNA (D-001206-13-20, Dharmacon, Horizon Discovery, Cambridge, UK), TAZ-siRNA (M-041057-01-0010, Dharmacon), or Nr4a1-siRNA (L-040970-01-0005, Dharmacon) (25 nM) using DharmaFECT1 (T-2001-03, Dharmacon) were seeded on semipermeable filters of the Transwell system (0.4 μm pore size, Transwell Permeable Supports, catalog no. 3450, Corning, NY, USA) for 4 days until polarization and then incubated in serum-free and hormone-free medium for another 24 h before dDAVP treatment. The efficiency of siRNA-mediated KD was evaluated, and the data were presented in Figure S1. dDAVP (10⁻⁹ M) was applied to the basolateral side of mpkCCDc11 cells for the last 24 h.

2.5 | Real-Time Quantitative Polymerase Chain Reaction (RT-qPCR)

Total RNA was extracted using the Direct-zol RNA MiniPrep Kit (R2050, Zymo Research, Irvine, CA), according to the manufacturer's protocol. cDNA was synthesized from 500 ng of total RNA using the PrimeScript 1st Strand cDNA Synthesis Kit (6110A, Takara, Kusatsu, Shiga, Japan), according to the manufacturer's instructions. RT-qPCR was performed using the QuantiTECT SYBR Green PCR Kit (204143, QIAGEN) to assess the relative expression of the target genes. β-actin mRNA was used as an internal control. RT-qPCR was performed on Rotor-Gene-A (QIAGEN) and the threshold was set by 0.02 to determine the threshold cycle (Ct) value. Relative mRNA expression was assessed as described previously [31]. The primers were designed by OriGene (Rockville, MD, USA) and purchased from Macrogen (Seoul, Korea). Each sample was tested in duplicate. The primer sequences used for RT-qPCR are presented in Table 1.

2.6 | cAMP Measurement

Intracellular cAMP levels were measured in mpkCCDc11 cells as previously described [34]. Cells were cultured to confluence in a 6-well Transwell system (0.4 μm pore size, Transwell Permeable Supports, 3450, Corning) for 4 days and starved for the next 24 h. After preincubation with 1 mM 3-isobutyl-1-methylxanthine (IBMX; I5879, Sigma) for 10 min to inhibit cyclic nucleotide

TABLE 1 | Primer sequences for quantitative real-time PCR.

Primer		Sequence
<i>Aqp2</i>	Forward	5'-GCCATCCTCCATGAGATTACCC-3'
	Reverse	5'-CGCTCATCAGTGGAGGCAAAGA-3'
<i>TAZ</i>	Forward	5'-GTCACCAACAGTAGCTCAGATCC-3'
	Reverse	5'-GTTGCTGAGGAAGTCTTCTGGAG-3'
<i>Nr4a1</i>	Forward	5'-GTGCAGTCTGTGGTGACAATGC-3'
	Reverse	5'-CAGGCAGATGTACTTGGCGCTT-3'
<i>Cebpb</i>	Forward	5'-CAACCTGGAGACGCAGCACAAG-3'
	Reverse	5'-GCTTGAACAAGTCCGCAGGGT-3'
<i>Mef2d</i>	Forward	5'-GGTTTCCGTGGCAACACCAAGT-3'
	Reverse	5'-GCAGGTGAAGTGAAGGCTGGTA-3'
<i>Elf3</i>	Forward	5'-TCCTCCGACTACCTTTGGCACT-3'
	Reverse	5'-ACTCCAGAACCTGGGTCTTCGA-3'
<i>Klf5</i>	Forward	5'-AGCTCACCTGAGGACTCATAACG-3'
	Reverse	5'-AGAAGCTGCGTTGGCACACCAT-3'
<i>Junb</i>	Forward	5'-GACCTGCACAAGATGAACCACG-3'
	Reverse	5'-ACTGCTGAGGTTGGTGTAGACG-3'
<i>Stat3</i>	Forward	5'-AGGAGTCTAACACGGCAGCCT-3'
	Reverse	5'-GTGGTACACCTCAGTCTCGAAG-3'

phosphodiesterase, vehicle or dDAVP (10^{-9} M) was added for 15 min in the presence of IBMX. The intracellular cAMP levels were determined using a competitive enzyme immunoassay (501040, Cayman Chemical, Ann Arbor, MI, USA) according to the manufacturer's instructions. The results were expressed in picomoles per milliliter of cell lysate.

2.7 | Cell Counting Kit (CCK)-8 Cell Proliferation Assay

mpkCCDC11 cells transfected with control-siRNA or TAZ-siRNA were seeded on 96-well culture plates at a density of 1×10^4 cells per well. After incubation for 24 h in a humidified incubator at 37°C with 5% CO_2 , the CCK-8 assay was performed according to the manufacturer's instructions [35]. Briefly, $10 \mu\text{L}$ of CCK-8 solution (CK04, Dojindo Molecular Technologies Inc., Rockville, MD, USA) was added to each well, followed by incubation for 3 h at 37°C . The absorbance was measured at a wavelength of 450 nm using a microplate reader.

2.8 | Immunohistochemistry and Immunocytochemistry

Left kidneys were fixed by transcardiac perfusion with 2% paraformaldehyde-lysine-periodate solution for 10 min. The kidneys were then embedded in poly (ethylene glycol) (400) disteate (Cat. no. 01048, Polysciences Inc.) and cut transversely at a thickness of $4 \mu\text{m}$ using a microtome. Immunolabeling was performed using the methods, as previously described [30]. Immunofluorescence microscopy was performed in cultured cells, as described previously [36]. For AQP2 immunolabeling, cultured cells were incubated with rabbit anti-AQP2 polyclonal antibody (1:100, AB3274, Merck Millipore) in PBS at 4°C overnight. Cells were washed and incubated with goat-anti-rabbit IgG Alexa Fluor 488 secondary antibody (A11008, Invitrogen) for 2 h at room temperature. Nuclei were stained with DAPI (D1306, Invitrogen) for 30 min at room temperature and cells were mounted with an antifading reagent (P36934, Invitrogen). Immunofluorescence microscopy was performed using a laser scanning confocal microscope (Zeiss LSM 800, Jena, Germany).

2.9 | RNA Sequencing

mpkCCDC11 cells were transfected with control-siRNA or TAZ-siRNA. After siRNA treatment for 5 days, dDAVP (10^{-9} M) treatment was performed for 24 h. Each experimental group included three independent cell preparations. For mRNA profiling, total RNA was extracted from mpkCCDC11 cells treated with siRNA and was used for preparation of cDNA library. cDNA libraries were generated using the TruSeq Stranded mRNA Library Prep Kit according to the manufacturer's protocol (TruSeq Stranded mRNA Reference Guide #1000000040498v00, Illumina, San Diego, CA, USA). The libraries were pooled and sequenced on the Illumina NovaSeq platform, achieving a depth of more than 40 million reads (100-bp paired-end reads) per sample. The mouse GRCh39 genome reference assembly was used to map sequence reads. The quality of the sequence reads was assessed using FastQC (Babraham Bioinformatics, Babraham Institute,

Cambridge, UK). Trimmed reads were mapped to the reference genome using HISAT2 [37] after pre-processing. Genomic and transcriptomic assemblies were obtained using the StringTie program [38] based on the reference gene model. Subsequently, transcript abundance was quantified using read counts and normalized values, including transcripts per million (TPM), were calculated. KEGG pathway enrichment analysis was performed in significantly differentially expressed genes (DEGs, Benjamini-Hochberg-adjusted $p < 0.05$) from each comparison. KEGG pathways were identified on the Metascape platform [39]. To avoid a sample source bias in the pathway enrichment analysis, total genes with the considerable transcript abundance were considered as a background gene set. All raw files generated from RNA-Seq are available in NCBI's Gene Expression Omnibus (GSE274937, <https://www.ncbi.nlm.nih.gov/geo/query/acc.cgi?acc=GSE274937>).

2.10 | Statistical Analysis

Quantitative data are presented as means \pm standard errors of the means (SEMs). Comparisons between the two groups were performed using the unpaired *t*-test. Multiple groups were compared using one-way analysis of variance (ANOVA), followed by Tukey's multiple comparison test. GraphPad Prism software (GraphPad) was used for all statistical analyses. *p* values of < 0.05 were considered statistically significant. The significance of differential gene expression was considered if the adjusted *p* value, as determined by Benjamini-Hochberg correction of *p* values, was < 0.05 .

3 | Results

3.1 | Changes in AQP2 Expression and Urine Output in Collecting Duct-Specific TAZ-Knockout Mice

To investigate the effects of TAZ depletion in kidney collecting ducts on AQP2 expression and urine output, we analyzed collecting duct-specific TAZ-knockout mice (TAZ^{fl/fl}; HoxB7Cre) and control mice (TAZ^{fl/fl}). Semiquantitative immunoblotting of kidney cortical lysates showed no significant reduction in TAZ protein levels in the TAZ^{fl/fl}; HoxB7Cre mice (Figure 1A,D). This lack of reduction may be attributed to the broad distribution pattern of the *Wwtr1* gene, which is expressed throughout all 14 tubular segments of the mouse kidney (<https://esbl.nhlbi.nih.gov/MRECA/Nephron/>). However, AQP2 protein abundance was markedly decreased in the COR ($24\% \pm 4\%$ of TAZ^{fl/fl} mice, $p < 0.05$, Figure 1A,E) and OM ($46\% \pm 4\%$ of TAZ^{fl/fl} mice, $p < 0.05$, Figure 1B,F) of TAZ^{fl/fl}; HoxB7Cre mice. In contrast, AQP2 protein levels in the IM remained unchanged (Figure 1C,G). Consistent with the decreased AQP2 protein abundance in the COR and OM, knockout mice exhibited a significant increase in urine output (4.33 ± 1.53 mL/day vs. 0.56 ± 0.37 mL/day in TAZ^{fl/fl} mice, $p < 0.05$).

Immunoperoxidase labeling further demonstrated reduced AQP2 intensity in the kidney COR (i.e., connecting tubule and cortical collecting duct) of TAZ^{fl/fl}; HoxB7Cre mice (Figure 2A,B). In contrast, AQP2 immunolabeling intensity in the OM and IM

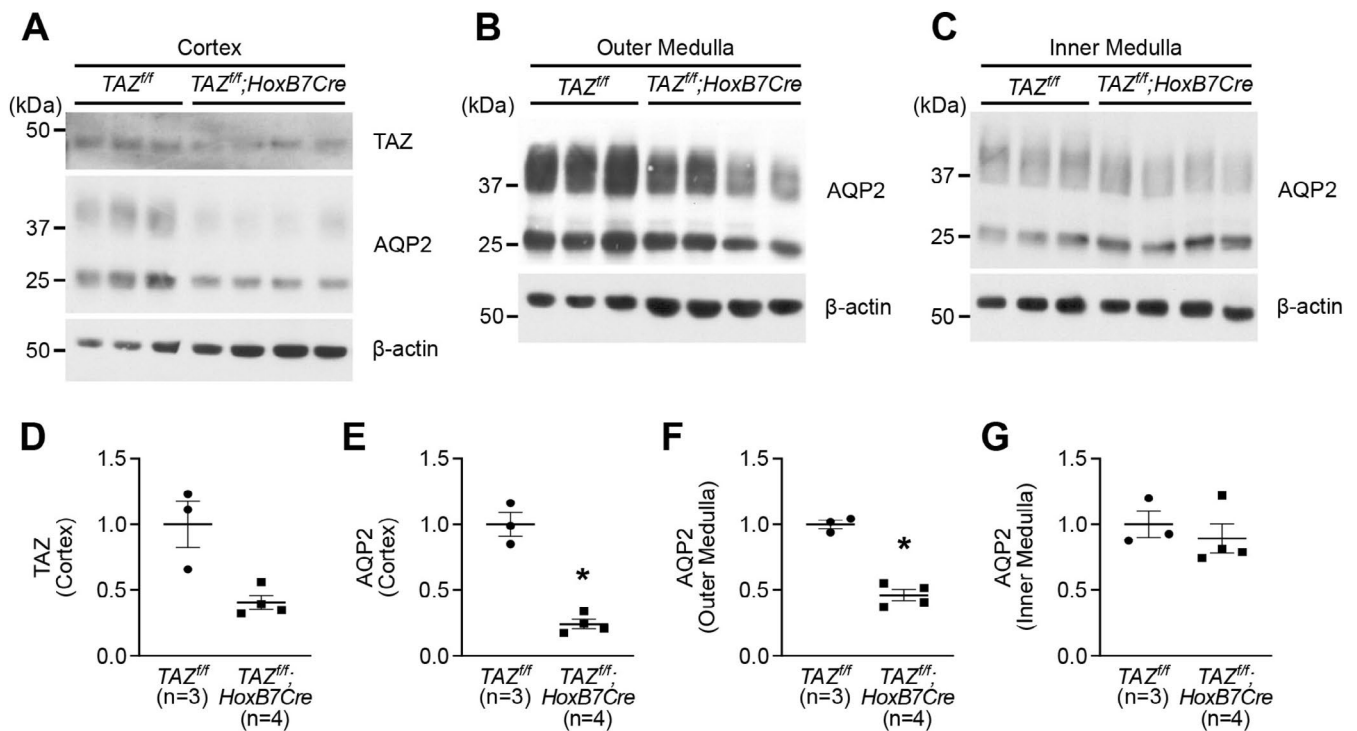


FIGURE 1 | Semiquantitative immunoblotting in kidney lysates from control ($TAZ^{fl/fl}$) and collecting duct-specific TAZ-knockout ($TAZ^{fl/fl}; HoxB7Cre$) mice. Representative immunoblots (A–C) and corresponding graphs showing protein quantification (D–G) for TAZ and AQP2 in different kidney regions (cortex, outer medulla, and inner medulla). β -Actin was used as a loading control. n , the number of mice in each group. $*p < 0.05$ compared with $TAZ^{fl/fl}$.

showed no differences between groups (Figure 2C–F). No apparent structural alterations in collecting ducts were observed (Figure 2).

3.2 | Changes in Vasopressin-Induced *Aqp2* Expression by TAZ Knockdown in mpkCCDc11 Cells

The effects of siRNA-mediated TAZ-knockdown (TAZ-KD) on AQP2 protein and mRNA expression in response to vasopressin (dDAVP) treatment were evaluated in mpkCCDc11 cells using semiquantitative immunoblotting and RT-qPCR. TAZ-siRNA treatment significantly reduced total TAZ protein abundance compared to control-siRNA-treated cells ($43\% \pm 5\%$ of vehicle group treated with control-siRNA, $p < 0.05$) and this reduction persisted with dDAVP treatment ($32\% \pm 3\%$ of vehicle group treated with control-siRNA, $p < 0.05$ Figure 3A,B). Phosphorylated TAZ (Ser89) protein levels (measured as the ratio of phosphorylated TAZ to total TAZ) remained unchanged after TAZ-KD (Figure 1A,C); however, dDAVP treatment induced phosphorylated TAZ (Ser89) levels ($152\% \pm 14\%$ of vehicle group treated with control-siRNA, $p < 0.05$ Figure 3A,C), suggesting TAZ inactivation and decreased cellular activities [40].

In control-siRNA-treated cells, dDAVP (10^{-9} M, 24 h) significantly increased AQP2 protein abundance to $287\% \pm 15\%$ of vehicle-treated cells ($p < 0.05$, Figure 3A,D). dDAVP (10^{-9} M, 24 h) also increased AQP2 protein abundance in TAZ-KD cells when compared to vehicle-treated TAZ-KD cells ($214\% \pm 22\%$, $p < 0.05$, Figure 3A,D). However, dDAVP-responsive induction

of AQP2 was significantly attenuated in TAZ-KD cells, when compared to control-siRNA-treated cells ($p < 0.05$, Figure 3A,D). Similarly, RT-qPCR revealed that dDAVP increased *Aqp2* mRNA expression to $12,608\% \pm 165\%$ of vehicle-treated levels in control-siRNA-treated cells ($p < 0.05$, Figure 3E). Moreover, dDAVP increased *Aqp2* mRNA expression to $914\% \pm 24\%$ of vehicle-treated levels in TAZ-KD cells ($p < 0.05$, Figure 3E). However, dDAVP-responsive induction of *Aqp2* mRNA levels was significantly blunted in TAZ-KD cells, when compared to control-siRNA-treated cells ($p < 0.05$, Figure 3E). Despite the reduced dDAVP response in AQP2 levels, the findings indicate that TAZ-KD did not abolish vasopressin-induced AQP2 expression at either the mRNA or protein levels. Importantly, cAMP levels measured after dDAVP stimulation were comparable between control-siRNA- and TAZ-siRNA-treated cells (Figure 3F), indicating that the observed effects were independent of cAMP production. In addition, a significant decrease in cell proliferation assessed by CCK-8 assay was observed in TAZ-siRNA-treated mpkCCDc11 cells, when compared to both untreated and control-siRNA-treated cells ($73\% \pm 1\%$ of untreated cells, $p < 0.05$, Figure 3G).

Immunocytochemical analysis supported these findings: dDAVP significantly increased AQP2 immunolabeling intensity in control-siRNA-treated cells but not in TAZ-KD cells (Figure 4A–D vs. Figure 4G–J). These results demonstrate that TAZ plays a role in mediating vasopressin-induced transcriptional upregulation of *Aqp2*. Despite TAZ knockdown, dDAVP stimulation continued to induce AQP2 targeting to the plasma membrane (Figure 4J,L), likely through cAMP pathways that remain unaffected by TAZ-KD. The findings suggest that TAZ

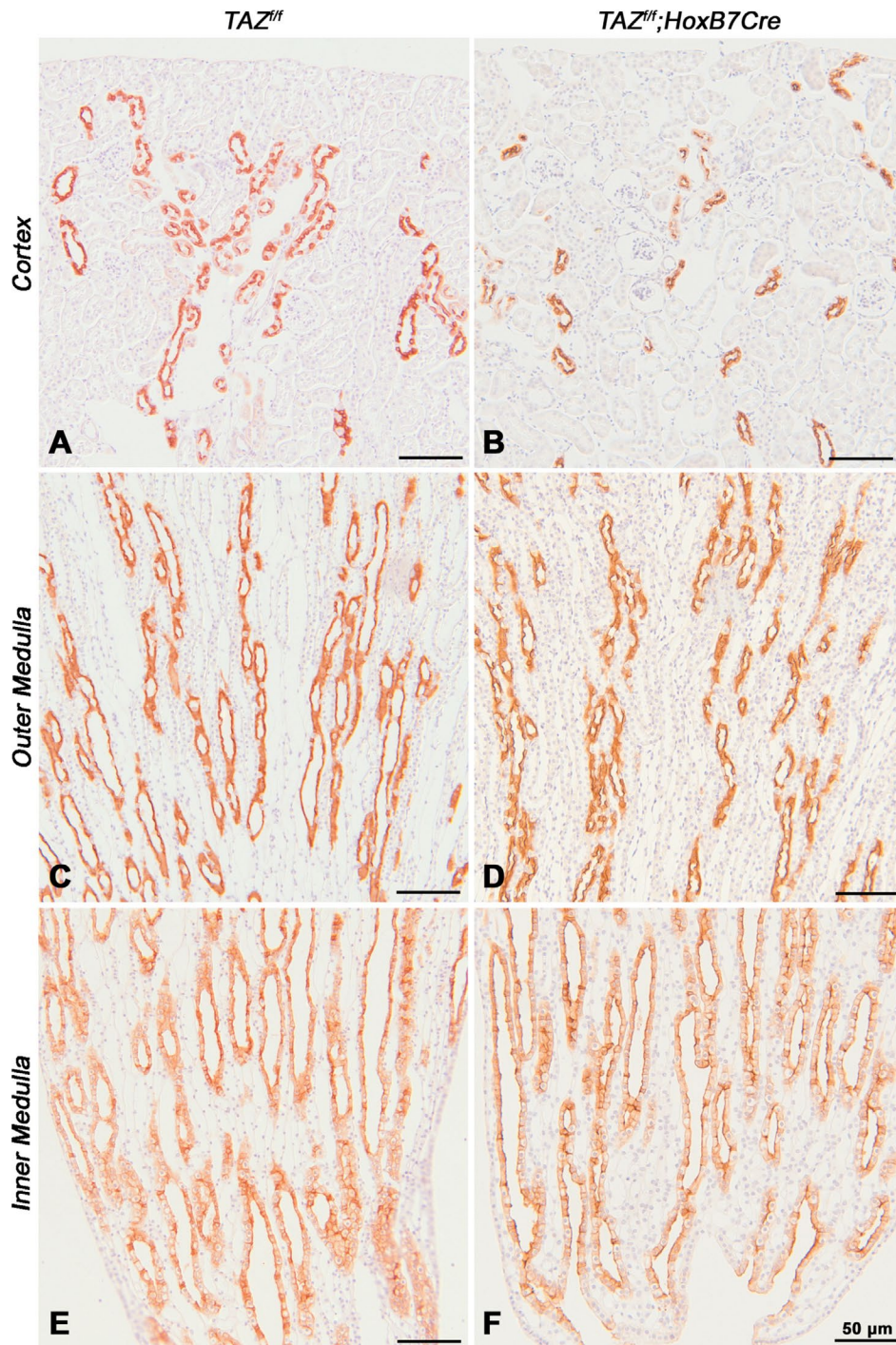


FIGURE 2 | Immunoperoxidase labeling for AQP2 in the kidney tissue sections from control ($TAZ^{fl/fl}$) and collecting duct-specific TAZ-knockout ($TAZ^{fl/fl}; HoxB7Cre$) mice. Representative images from the cortex (A, B), outer medulla (C, D), and inner medulla (E, F) are shown. Scale bars ($50\mu m$) are included in each panel.

may not significantly influence the short-term trafficking mechanism of AQP2.

3.3 | Transcription Factors Associated With *Aqp2* Expression in Genome-Wide Transcriptome Profiles

TAZ functions as a transcriptional coactivator for numerous genes; however, its role in *Aqp2* transcription remains unclear.

To address this, RNA-Seq was performed to analyze genome-wide transcriptomic changes in mpkCCDC11 cells following TAZ-KD under vehicle or dDAVP treatment ($10^{-9}M$, 24h) to identify DEGs associated with *Aqp2* transcription.

The transcriptomic response to dDAVP treatment ($10^{-9}M$, 24h) was visualized using a volcano plot, demonstrating significantly altered genes (adjusted $p < 0.05$, blue), including *Aqp2* (Figure 5A). The RNA-Seq dataset validated the robust response of mpkCCDC11

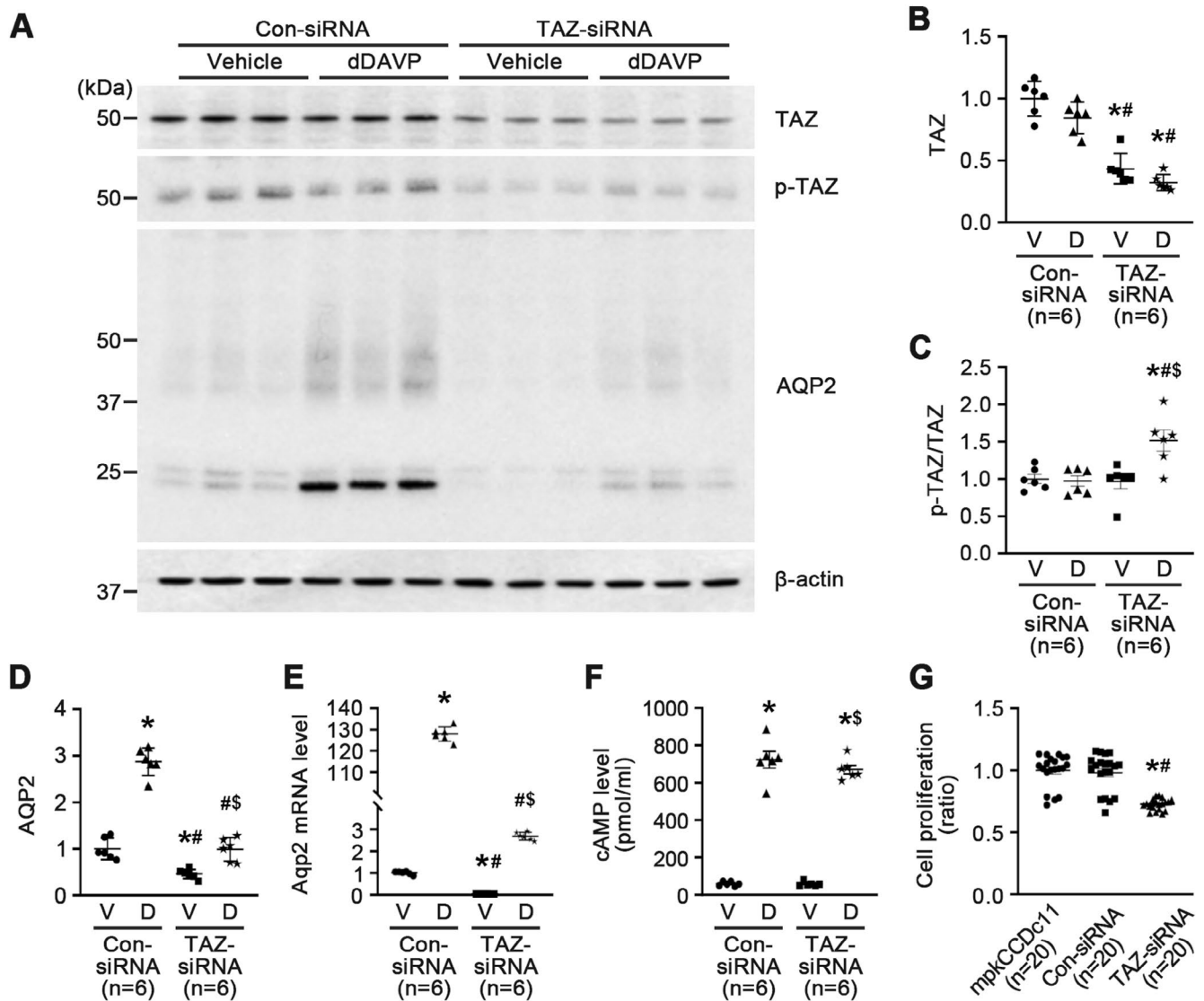


FIGURE 3 | Semi-quantitative immunoblotting and real-time quantitative polymerase chain reaction (RT-qPCR) analysis of mpkCCDc11 cells treated with control-siRNA or TAZ-siRNA in the absence or presence of dDAVP (10^{-9} M, 24 h). (A–D) The immunoblots were reacted with antibodies against AQP2 (~25 kDa deglycosylated AQP2 and ~37–50 kDa glycosylated AQP2), TAZ (~49 kDa), phosphorylated TAZ (p-TAZ, ~49 kDa), and β -Actin (~42 kDa, loading control). (E) Changes in Aqp2 mRNA level in mpkCCDc11 cells. (F) cAMP levels in mpkCCDc11 cells treated with control-siRNA or TAZ-siRNA in the absence or presence of dDAVP (10^{-9} M, 24 h). (G) Cell proliferation assay (CCK-8) of mpkCCDc11 cells (untreated) and mpkCCDc11 cells treated with control-siRNA (Con-siRNA) or TAZ-siRNA. * $p < 0.05$ compared with the vehicle group treated with control-siRNA. # $p < 0.05$ compared with the dDAVP group treated with control-siRNA. \$ $p < 0.05$ compared with the vehicle group treated with TAZ-siRNA. D, dDAVP; n, the number of independent cell preparations in each group; V, vehicle.

cells to dDAVP by identifying several known dDAVP-responsive genes from previous studies [11, 41]. Based on a prior study by Kikuchi et al. [11], which identified 17 candidate TFs potentially involved in vasopressin-induced *Aqp2* regulation via genomic regulatory elements, the differential expression of these TFs was assessed in the current RNA-Seq dataset (Figure 5B). Among the 17 TFs, seven (*Nr4a1*, *Cebpb*, *Mef2d*, *Elf3*, *Klf5*, *Junb*, *Stat3*) were significantly upregulated by dDAVP in either control or TAZ-KD conditions (Figure 5B, Table 2). Among them, to identify TAZ-dependent TFs exhibiting attenuated expression in TAZ-KD cells following dDAVP stimulation, RT-qPCR analysis was performed (Figure 5C–J). RT-qPCR validation confirmed a significant reduction in *Nr4a1* mRNA levels under TAZ-KD conditions following dDAVP stimulation compared to controls (Figure 5D). In contrast,

mRNA levels of other TFs (*Cebpb*, *Mef2d*, *Elf3*, *Klf5*, *Junb*, *Stat3*) were unaltered (Figure 5E–J), implicating that *Nr4a1* emerged as a key TAZ-dependent regulator required for dDAVP-induced AQP2 expression.

3.4 | NR4A1 Expression in the Cytoplasmic and Nuclear Extracts of mpkCCDc11 Cells Following dDAVP Treatment Under TAZ-KD

mpkCCDc11 cells were transfected with control-siRNA or TAZ-siRNA and subsequently were treated with vehicle or dDAVP (10^{-9} M, 24 h). Cytoplasmic and nuclear protein fractions were then isolated for analysis. At baseline, TAZ was detected in

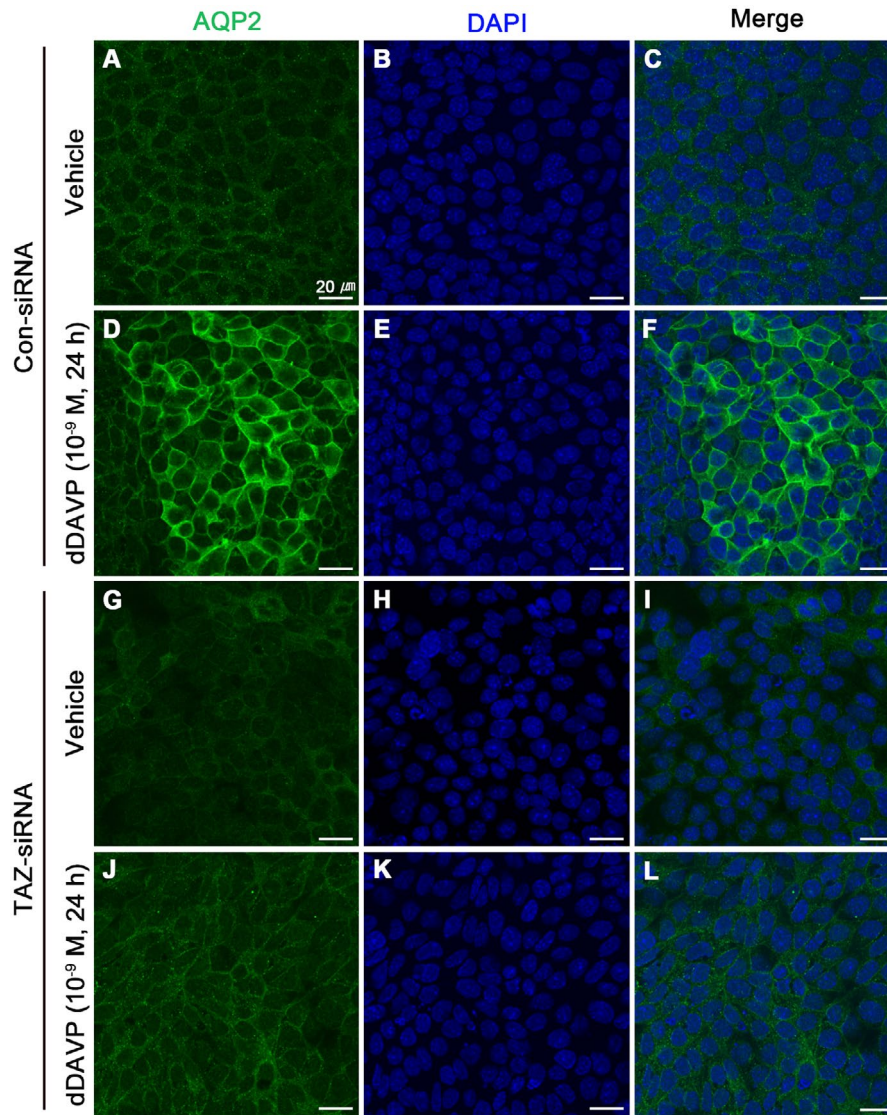


FIGURE 4 | Immunofluorescence microscopic examination of AQP2 in mpkCCDc11 cells treated with control-siRNA (A–F) or TAZ-siRNA (G–L) in the absence or presence of dDAVP (10^{-9} M, 24 h). Nuclei were counterstained with 4',6-diamidino-2-phenylindole (DAPI). Scale bars, 20 μ m.

both cytoplasmic and nuclear fractions of mpkCCDc11 cells, with higher abundance in the nuclear fraction (Figure 6). TAZ-siRNA transfection effectively reduced TAZ protein levels in both cytoplasmic (Figure 6A,B) and nuclear (Figure 6A,C) fractions. dDAVP treatment for 24 h did not affect TAZ abundance in either subcellular compartment (Figure 6A–C). In contrast to TAZ, immunoblotting revealed that NR4A1 was exclusively localized to the nuclear fraction in mpkCCDc11 cells (indicated by arrow Figure 6A). Following dDAVP stimulation (10^{-9} M, 24 h), nuclear NR4A1 protein levels were significantly upregulated in control-siRNA-transfected cells ($380\% \pm 66\%$, $p < 0.05$, Figure 6A,D). However, this dDAVP-induced NR4A1 upregulation was abolished in TAZ-siRNA-treated cells (Figure 6A,D).

3.5 | Changes in AQP2 Expression After Nr4a1 Knockdown

To investigate whether NR4A1 directly contributes to dDAVP-induced AQP2 expression, *Nr4a1* knockdown (Nr4a1-KD) was

performed using siRNA transfection in mpkCCDc11 cells. Although semiquantitative immunoblotting showed no significant reduction in NR4A1 protein levels after Nr4a1-siRNA treatment compared to controls ($91\% \pm 5\%$, n.s. [not significant], Figure 7A,B), RT-qPCR confirmed a significant reduction in *Nr4a1* mRNA levels ($53\% \pm 3\%$, $p < 0.05$; Figure 7C), indicating effective transcript-level silencing despite residual protein expression. The discrepancy between NR4A1 protein and mRNA levels after siRNA-mediated knockdown may result from residual protein expression or the limited sensitivity of immunoblotting.

dDAVP stimulation significantly increased NR4A1 protein abundance in control-siRNA-treated cells but induced a smaller increase in Nr4a1-KD cells (Figure 7A,B). The protein expression of TAZ was unaffected by Nr4a1-KD under vehicle or dDAVP stimulation (10^{-9} M, 24 h, Figure 7A,F). Importantly, Nr4a1-KD significantly attenuated the dDAVP-induced increase in AQP2 protein abundance compared to controls (Figure 7A,D). Similarly, RT-qPCR revealed reduced

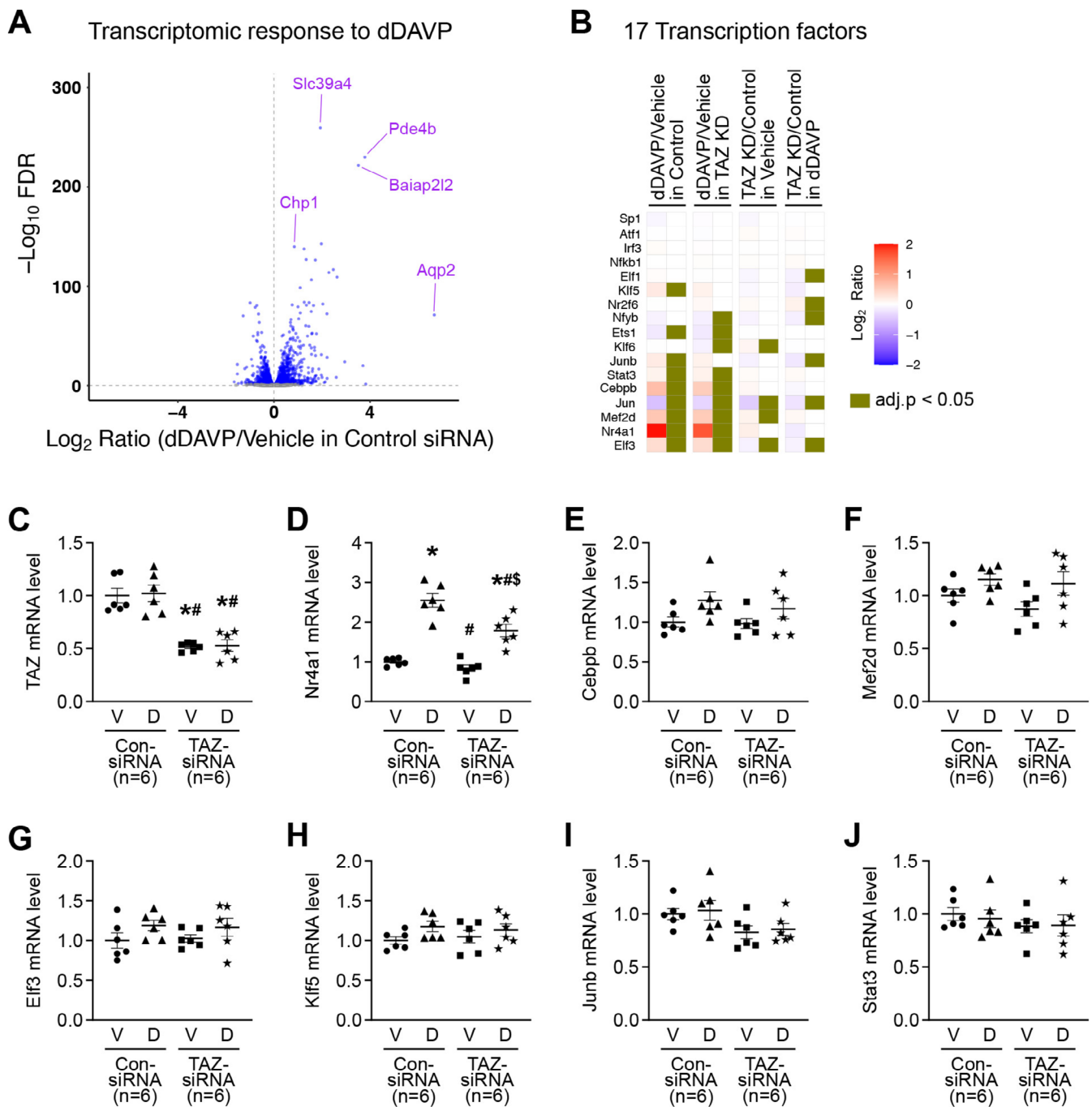


FIGURE 5 | RNA-Sequencing (RNA-Seq) and real-time quantitative polymerase chain reaction (RT-qPCR) of transcription factor (TF) candidates in mpkCCDc11 cells treated with control-siRNA or TAZ-siRNA under vehicle or dDAVP stimulation (10^{-9} M, 24h). (A–H) (A) Volcano plot illustrating dDAVP-responsive transcriptomic changes in mpkCCDc11 cells treated with control-siRNA. Significantly altered genes (blue) were defined by an adjusted $p < 0.05$. Vasopressin-regulated genes exhibiting robust transcriptomic changes (e.g., *Aqp2*, *Pde4b*, *Baiap2l2*, *Slc39a4*, and *Chp1*) were labeled. (B) Heatmap showing expression changes of 17 TFs potentially involved in *Aqp2* transcription in mpkCCDc11 cells treated with control-siRNA or TAZ-siRNA under vehicle or dDAVP conditions (10^{-9} M, 24h). TF genes were listed with expression changes (color gradient scale) and statistical significance ($\text{adj.} p < 0.05$). (C–J) RT-qPCR analysis of mRNA expression levels for TAZ and 7 TFs (*Nr4a1*, *Cebpb*, *Mef2d*, *Eif3*, *Klf5*, *Junb*, *Stat3*). * $p < 0.05$ compared with the vehicle group treated with control-siRNA. # $p < 0.05$ compared with the dDAVP group treated with control-siRNA. \$ $p < 0.05$ compared with the vehicle group treated with TAZ-siRNA. D, dDAVP; n, the number of cell preparations in each group; V, vehicle.

dDAVP-induced *Aqp2* mRNA expression following *Nr4a1*-KD (Figure 7E). These results indicate that NR4A1 is essential for vasopressin-induced AQP2 expression. Additionally, *Nr4a1*-KD did not affect the dDAVP-induced increase in intracellular cAMP levels (Figure 7G), indicating that the observed effects were independent of cAMP production.

3.6 | Cellular Pathways Associated With dDAVP- and TAZ-Dependent Genes

KEGG pathway enrichment analysis was performed on DEGs across three comparisons, (1) TAZ-KD versus Control-siRNA under vehicle treatment; (2) TAZ-KD versus Control-siRNA

TABLE 2 | The 17 transcription factors with the greatest likelihood of mediating vasopressin-dependent increases in *Aqp2* transcription.

Rank	Gene symbol	Description	Fold change (log ₂ -based ratio)			
			Con_dDAVP/ Con_Vehicle	TAZ_dDAVP/ TAZ_Vehicle	TAZ_Vehicle/ Con_Vehicle	TAZ_dDAVP/ Con_dDAVP
1	<i>Nr4a1</i>	Nuclear receptor subfamily 4, group A, member 1	1.972*	1.632*	0.166	-0.173
2	<i>Cebpb</i>	CCAAT/enhancer binding protein (C/EBP), beta	0.673*	0.527*	0.079	-0.066
3	<i>Mef2d</i>	Myocyte enhancer factor 2D	0.586*	0.536*	0.127*	0.077
4	<i>Elf3</i>	E74-like factor 3	0.352*	0.362*	-0.121*	-0.111*
5	<i>Klf5</i>	Kruppel-like factor 5	0.226*	0.143	-0.060	-0.143
6	<i>Junb</i>	Jun B proto-oncogene	0.214*	0.141	-0.129	-0.201*
7	<i>Stat3</i>	Signal transducer and activator of transcription 3	0.130*	0.139*	0.045	0.054
8	<i>Irf3</i>	Interferon regulatory factor 3	0.036	0.018	0.010	-0.007
9	<i>Elf1</i>	E74-like factor 1	0.031	-0.008	-0.077	-0.116*
10	<i>Nfkb1</i>	Nuclear factor of kappa light polypeptide gene enhancer in B cells 1, p105	0.003	0.024	0.022	0.042
11	<i>Klf6</i>	Kruppel-like factor 6	-0.007	-0.116*	0.092*	-0.018
12	<i>Nr2f6</i>	Nuclear receptor subfamily 2, group F, member 6	-0.010	0.072	0.062	0.144*
13	<i>Atf1</i>	Activating transcription factor 1	-0.016	-0.027	0.043	0.032
14	<i>Sp1</i>	Trans-acting transcription factor 1	-0.073	-0.022	-0.064	-0.013
15	<i>Nfyb</i>	Nuclear transcription factor-Y beta	-0.108	-0.139*	-0.105	-0.136*
16	<i>Ets1</i>	E26 avian leukemia oncogene 1, 5' domain	-0.187*	-0.187*	-0.004	-0.004
17	<i>Jun</i>	Jun proto-oncogene	-0.543*	-0.355*	-0.422*	-0.235*

*Adjusted $p < 0.05$.

under dDAVP treatment; (3) dDAVP versus vehicle in TAZ-KD. The analysis effectively identified cellular pathways significantly regulated by TAZ-KD (Figure 8A). Five KEGG pathways were identified as common pathways across all three comparisons. However, focusing on the pathways specifically altered by TAZ-KD, “HIF-1 signaling,” “Renal Cell Carcinoma,” and “Glycolysis/Gluconeogenesis” emerged as the key cellular pathways directly associated with TAZ. These three pathways have previously been reported as TAZ-involved cellular pathways [42–45], supporting the consistency of TAZ-dependent genes identified in this study with known TAZ targets. In addition, two other KEGG pathways, “Focal adhesion” and “ECM-receptor

interaction,” were enriched among genes responsive to dDAVP treatment in TAZ-KD cells, suggesting they are more influenced by vasopressin signaling than by direct TAZ regulation.

Figure 8B provides detailed insights into how TAZ-KD impacts genes within the identified pathways. Downregulation of pathway-associated genes following TAZ-KD suggested that TAZ positively regulates these pathways. Moreover, genes that were decreased with TAZ-KD but increased with dDAVP treatment highlight potential targets for further study into TAZ-mediated regulatory mechanisms associated with vasopressin signaling of kidney collecting duct cells.

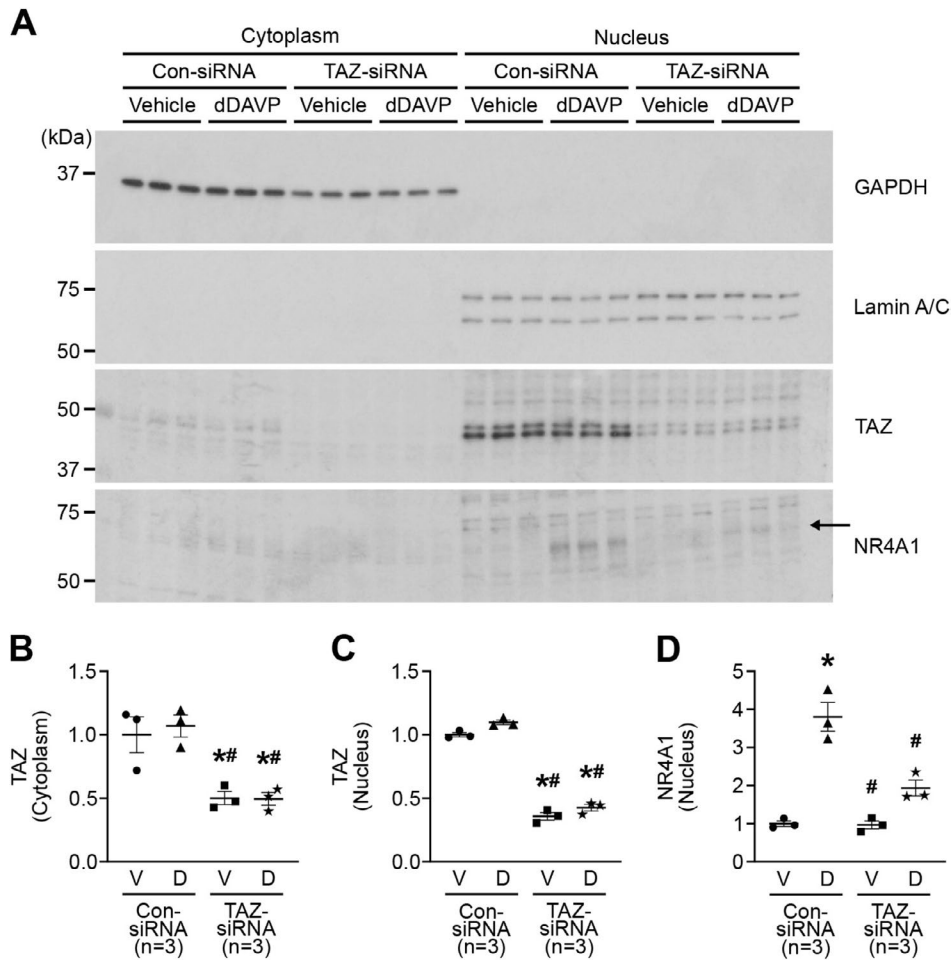


FIGURE 6 | Semi-quantitative immunoblotting of TAZ and NR4A1 in the cytoplasmic and nuclear extracts of mpkCCDc11 cells following vehicle or dDAVP treatment under control-siRNA- or TAZ-siRNA-mediated knockdown. (A) The immunoblots were reacted with primary antibodies against TAZ (~49 kDa), NR4A1 (~64 kDa), GAPDH (~37 kDa), and Lamin A/C (~74 kDa Lamin A and ~63 kDa Lamin C). (B–D) Changes in TAZ (B, cytoplasm; C, nucleus) and NR4A1 (D, nucleus) levels in mpkCCDc11 cells treated with control-siRNA or TAZ-siRNA in the absence or presence of dDAVP (10^{-9} M, 24 h). * $p < 0.05$ compared with the vehicle group treated with control-siRNA. # $p < 0.05$ compared with the dDAVP group treated with control-siRNA. D, dDAVP; n, the number of cell preparations in each group; V, vehicle.

4 | Discussion

Our findings demonstrate that TAZ is a novel regulatory factor of AQP2 expression. The collecting duct-specific TAZ-knockout mice exhibit polyuria and a significant reduction in AQP2 expression in the kidney cortex and outer medulla. Consistent with this, TAZ-KD in mpkCCDc11 cells significantly reduced vasopressin-induced increases in both AQP2 protein and mRNA levels, highlighting its essential role in water reabsorption. Furthermore, we identified NR4A1 as a TAZ-dependent TF that contributes to *Aqp2* expression. These findings provide new insights into the regulatory network governing water reabsorption in the kidney collecting duct.

The transcriptional regulation of *Aqp2* is essential for maintaining water balance and urine concentration. Vasopressin selectively enhances *Aqp2* gene transcription, as evidenced by previous studies showing increased RNA polymerase II binding to the *Aqp2* gene body in response to vasopressin stimulation [12]. This effect is highly selective, with only 35 of 3659 genes exhibiting vasopressin-dependent regulation [12]. The current study hypothesizes that YAP/TAZ, a component of the

Hippo signaling pathway, functions as a signal transducer in the initial response to extracellular stimuli (e.g., vasopressin). Therefore, initial response factors might not be detected in transient (short-term) transcriptomic changes that reflect secondary downstream effects. TAZ, a transcriptional coactivator structurally similar to YAP, is known to modulate gene expression by interacting with a variety of TFs rather than binding DNA directly. Thus, its regulatory effects may be largely mediated by various TFs as part of a cascade, which could explain why TAZ was not highlighted in previous ChIP-Seq or RNA-Seq studies that focused on direct transcriptional targets. Our results showed that TAZ-KD significantly attenuated dDAVP-induced increases in AQP2 protein and mRNA levels, suggesting that TAZ facilitates vasopressin-induced transcriptional regulation of *Aqp2*.

TAZ functions as a transcriptional coactivator by interacting with DNA-binding TFs such as TEADs. Previous studies have shown that TEAD-binding sites are critical for TAZ-mediated gene regulation [46, 47]. Although our study did not directly examine TEAD involvement, it is plausible that TAZ may regulate *Aqp2* transcription through interactions with TEAD or other

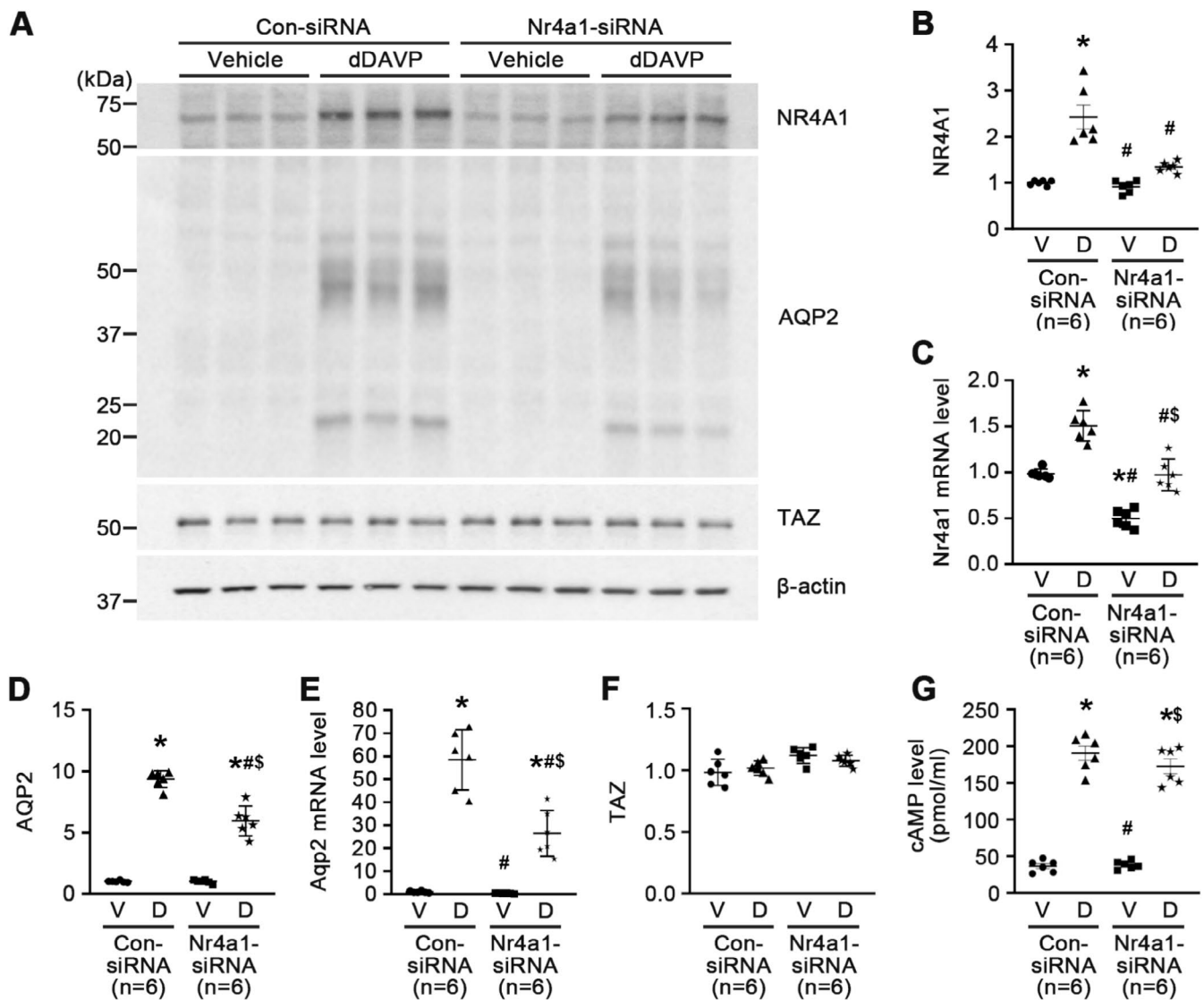


FIGURE 7 | Semi-quantitative immunoblotting and real-time quantitative polymerase chain reaction analysis of mpkCCDc11 cells treated with control-siRNA or Nr4a1-siRNA in the absence or presence of dDAVP (10^{-9} M, 24 h). (A, B, D, F) The immunoblots were reacted with primary antibodies against NR4A1 (~64 kDa), AQP2 (~25 kDa deglycosylated AQP2 and ~37–50 kDa glycosylated AQP2), TAZ (~49 kDa), and β -Actin (~42 kDa). (C, E) Changes in Nr4a1 or Aqp2 mRNA levels in mpkCCDc11 cells treated with control-siRNA or Nr4a1-siRNA in the absence or presence of dDAVP (10^{-9} M, 24 h). (G) cAMP levels in mpkCCDc11 cells treated with control-siRNA or Nr4a1-siRNA in the absence or presence of dDAVP (10^{-9} M, 24 h). * $p < 0.05$ compared with the vehicle group treated with control-siRNA. # $p < 0.05$ compared with the dDAVP group treated with control-siRNA. \$ $p < 0.05$ compared with the vehicle group treated with Nr4a1-siRNA. D, dDAVP; n, the number of cell preparations in each group; V, vehicle.

cofactors at enhancer or promoter regions of the *Aqp2* gene. Additionally, YAP, another Hippo pathway effector, has been shown to interact with GATA-family TFs (e.g., GATA2, GATA3) to enhance *Aqp2* expression [23]. This raises the possibility that TAZ may similarly collaborate with multiple TFs to regulate *Aqp2* expression. RNA-Seq analysis revealed that TAZ-KD under dDAVP stimulation downregulated several transcription factors (TFs), including *Elf3*, *Jun*, and *Junb* (Figure 5). These TFs have previously been implicated in vasopressin-induced gene regulation [11]. Among them, *Elf3* has been demonstrated to modulate both basal and vasopressin-stimulated *Aqp2* expression through its interaction with an Ets element in the promoter region [16]. Moreover, AP-1, a heterodimer composed of proteins from the *Jun* and *Fos* families, binds to the TPA response element (TRE) motifs in *Aqp2* promoter [18]. The observed downregulation of

key TFs such as *Elf3* and *Junb* following TAZ-KD underscores the central role of TAZ in coordinating complex transcriptional networks essential for vasopressin signaling. These findings suggest that TAZ not only regulates AQP2 expression but also coordinates broader transcriptional programs involved in renal physiology and vasopressin signaling.

An important aspect of this study is the identification of *Nr4a1* (*Nur77*) as a downstream effector of TAZ involved in regulating *Aqp2* expression. TAZ-KD significantly reduced dDAVP-induced *Nr4a1* mRNA expression (Figure 5D). A similar effect was observed at the protein level: dDAVP treatment markedly elevated NR4A1 protein abundance in the nuclear fraction of mpkCCDc11 cells, but the increase was abolished by TAZ-KD (Figure 6). Importantly, direct knockdown of

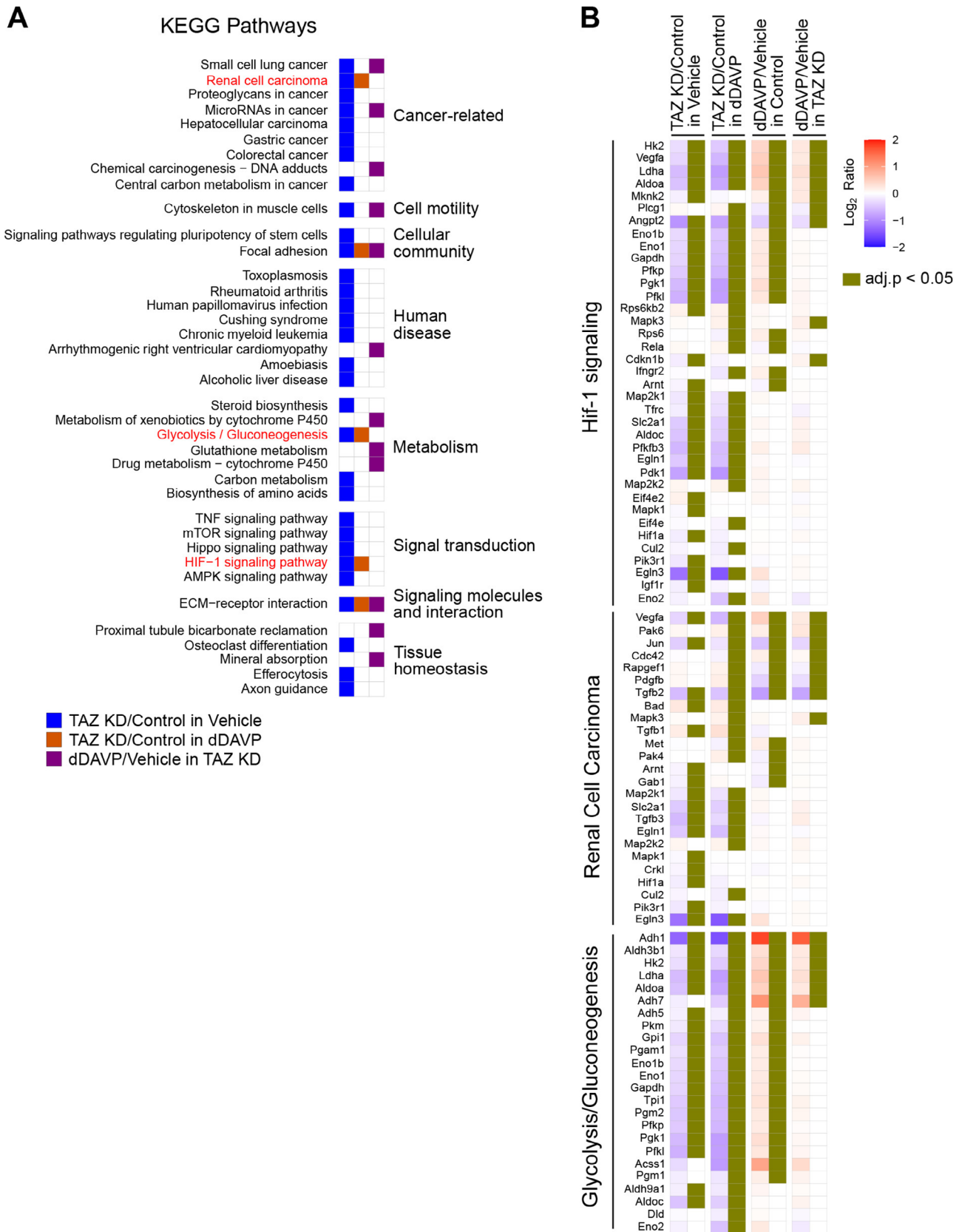


FIGURE 8 | KEGG pathways enrichment analysis of differentially expressed genes (DEGs) responsive to dDAVP and/or TAZ knockdown (KD). (A) Heatmap of KEGG pathways enriched by DEGs across three comparisons: (1) TAZ-KD versus control-siRNA under vehicle conditions; (2) TAZ-KD versus control-siRNA under dDAVP treatment; and (3) dDAVP versus vehicle in TAZ-KD cells. Pathways are classified by KEGG categories, and significance is indicated by adjusted $p < 0.05$. (B) Heatmaps illustrating transcriptomic changes for DEGs associated with three key KEGG pathways altered by TAZ-KD: “HIF-1 signaling,” “Renal Cell Carcinoma,” and “Glycolysis/Gluconeogenesis.” Expression changes are represented by a color gradient scale and statistical significance is indicated (adjusted $p < 0.05$).

Nr4a1 demonstrated its role in regulating AQP2: both protein and mRNA levels of AQP2 were significantly reduced after *Nr4a1*-KD under dDAVP stimulation (Figure 7). The finding suggests that TAZ regulates AQP2 abundance at least partially through its effect on *Nr4a1*. Previous studies have characterized *Nr4a1* as an immediate-early gene activated by diverse stimuli, including stress and growth factors [48–50]. In the kidney, *Nr4a1* has been implicated in processes such as fibrosis regulation via p38 MAPK signaling [51, 52]. While our data do not directly demonstrate NR4A1 binding to the *Aqp2* promoter or enhancer regions, prior evidence suggests that NR4A1 may function as a transcriptional activator in kidney-related conditions, for example, fibrosis and chronic kidney disease [51, 53]. Future studies using chromatin immunoprecipitation assays are needed to confirm whether NR4A1 directly interacts with regulatory elements of the *Aqp2* gene.

Beyond regulating AQP2 expression, TAZ affects many genes involved in cellular processes such as proliferation, differentiation, fibrosis, and cystogenesis [24, 54, 55]. Consistent with this, a significant reduction in cell proliferation (~30% compared to control) was observed following TAZ-KD. This finding implies that the observed decrease in baseline AQP2 levels may partly result from vasopressin-independent cellular alterations. TAZ is also known to interact with TEADs and other cofactors to regulate genes associated with epithelial-mesenchymal transition and extracellular matrix remodeling [54–56]. In our study, as shown in Figure 8, KEGG pathway enrichment analysis identified several pathways significantly affected by DEGs following TAZ-KD. Among these pathways, “HIF-1 signaling,” “Glycolysis/Gluconeogenesis,” and “Renal Cell Carcinoma” were directly associated with TAZ-mediated regulation. TAZ-mediated Hippo signaling is known to regulate these pathways through its effects on cellular metabolism and tumor progression [42–45]. Additionally, both TAZ and NR4A1 functionally interact with HIF-1 signaling in glucose metabolism [57, 58].

In particular, TAZ has been identified as a component of the PKD1-TAZ-Wnt- β -catenin-c-MYC signaling axis, which is essential for cystogenesis in PKD [24]. TAZ is highly expressed around renal cyst-lining epithelial cells in *Pkd1*-deficient mice, and deletion of TAZ in these mice significantly reduces cyst formation [24]. The connection between TAZ, *Nr4a1*, and AQP2 regulation may provide a potential mechanism in cyst formation and growth in PKD, as TAZ-dependent AQP2 regulation is likely to contribute to altered fluid secretion into cysts and accelerate their growth. Although NR4A1 has been identified as one of the targets of Hippo signaling in the regulation of proliferative and apoptotic processes [59], the direct functional interaction between TAZ and NR4A1 remains undefined. Further studies exploring the interactive regulation between TAZ and NR4A1 could provide novel insights into the functional roles of the TAZ-NR4A1 axis in vasopressin-responsive *Aqp2* transcription and cystogenesis.

In summary, this study demonstrates TAZ as a critical regulator of vasopressin-induced AQP2 expression through its transcriptional control of *Nr4a1*. Genome-wide transcriptomic analysis further highlights specific cellular pathways associated with TAZ-dependent gene regulation in kidney collecting duct cells. The findings offer novel insights into the molecular mechanisms

involved in the expression of AQP2 in response to vasopressin. Furthermore, the findings elucidate potential pathophysiological connections that may contribute to the progression of PKD, as TAZ is essential for cyst formation in PKD.

Author Contributions

H.S.C., H.-J.J., W.-Y.K., S.A.P., E.P., H.J.J., and T.-H.K. designed experiments; W.-Y.K. and S.A.P. performed experiments with knockout mice; H.S.C. and H.-J.J. performed in vitro experiments; H.-J.J., E.P., H.J.J., T.-H.K. performed RNA sequencing analysis; H.S.C., H.-J.J., W.-Y.K., S.A.P., E.P., H.J.J., and T.-H.K. analyzed the data and prepared the figures; H.S.C., H.-J.J., W.-Y.K., E.P., H.J.J., and T.-H.K. wrote the manuscript. All authors read and approved the final manuscript.

Acknowledgments

This work was supported by grants from the National Research Foundation of Korea (NRF) grant funded by the Korea Government (MIST) (RS-2021-NR060094; RS-2023-NR077104). H.J.J. was financially supported by the Edward S. Kraus Scholar Award, Johns Hopkins University School of Medicine Division of Nephrology.

Consent

All of the authors are aware of and agree to the content of the paper and their being listed as a coauthor of the paper.

Conflicts of Interest

The authors declare no conflicts of interest.

Data Availability Statement

All raw files generated from RNA-Sequencing are available in NCBI's Gene Expression Omnibus (GSE274937, <https://www.ncbi.nlm.nih.gov/geo/query/acc.cgi?acc=GSE274937>). The data that support the findings of this study are available in the Materials and Methods, Results, and/or Supporting Information of this article.

References

1. D. Bockenhauer and D. G. Bichet, “Pathophysiology, Diagnosis and Management of Nephrogenic Diabetes Insipidus,” *Nature Reviews. Nephrology* 11 (2015): 576–588.
2. E. Feraille, A. Sassi, V. Olivier, G. Arnoux, and P. Y. Martin, “Renal Water Transport in Health and Disease,” *Pflügers Archiv* 474 (2022): 841–852.
3. M. A. Knepper, T. H. Kwon, and S. Nielsen, “Molecular Physiology of Water Balance,” *New England Journal of Medicine* 372 (2015): 1349–1358.
4. W. Wang, C. Li, T. H. Kwon, M. A. Knepper, J. Frokiaer, and S. Nielsen, “AQP3, p-AQP2, and AQP2 Expression Is Reduced in Polyuric Rats With Hypercalcemia: Prevention by cAMP-PDE Inhibitors,” *American Journal of Physiology. Renal Physiology* 283 (2002): F1313–F1325.
5. M. D’Acerno, R. A. Fenton, and E. J. Hoorn, “The Biology of Water Homeostasis,” *Nephrology, Dialysis, Transplantation* 40 (2025): 632–640.
6. H. J. Jung and T. H. Kwon, “New Insights Into the Transcriptional Regulation of Aquaporin-2 and the Treatment of X-Linked Hereditary Nephrogenic Diabetes Insipidus,” *Kidney Research and Clinical Practice* 38 (2019): 145–158.
7. H. J. Jung and T. H. Kwon, “Molecular Mechanisms Regulating Aquaporin-2 in Kidney Collecting Duct,” *American Journal of Physiology. Renal Physiology* 311 (2016): F1318–F1328.

8. M. Centrone, M. Ranieri, A. Di Mise, et al., "AQP2 Trafficking in Health and Diseases: An Updated Overview," *International Journal of Biochemistry & Cell Biology* 149 (2022): 106261.
9. A. Kharin and E. Klussmann, "Many Kinases for Controlling the Water Channel Aquaporin-2," *Journal of Physiology* 602 (2024): 3025–3039.
10. R. A. Fenton, S. K. Murali, and H. B. Moeller, "Advances in Aquaporin-2 Trafficking Mechanisms and Their Implications for Treatment of Water Balance Disorders," *American Journal of Physiology. Cell Physiology* 319 (2020): C1–C10.
11. H. Kikuchi, H. J. Jung, V. Raghuram, et al., "Bayesian Identification of Candidate Transcription Factors for the Regulation of Aqp2 Gene Expression," *American Journal of Physiology. Renal Physiology* 321 (2021): F389–F401.
12. P. C. Sandoval, J. S. Claxton, J. W. Lee, F. Saeed, J. D. Hoffert, and M. A. Knepper, "Systems-Level Analysis Reveals Selective Regulation of Aqp2 Gene Expression by Vasopressin," *Scientific Reports* 6 (2016): 34863.
13. S. Uchida, Y. Matsumura, T. Rai, S. Sasaki, and F. Marumo, "Regulation of Aquaporin-2 Gene Transcription by GATA-3," *Biochemical and Biophysical Research Communications* 232 (1997): 65–68.
14. F. Petrillo, D. Chernyakov, C. Esteva-Font, S. B. Poulsen, B. Edemir, and R. A. Fenton, "Genetic Deletion of the Nuclear Factor of Activated T Cells 5 in Collecting Duct Principal Cells Causes Nephrogenic Diabetes Insipidus," *FASEB Journal* 36 (2022): e22583.
15. H. J. Jung, V. Raghuram, J. W. Lee, and M. A. Knepper, "Genome-Wide Mapping of DNA Accessibility and Binding Sites for CREB and C/EBPbeta in Vasopressin-Sensitive Collecting Duct Cells," *Journal of the American Society of Nephrology* 29 (2018): 1490–1500.
16. S. T. Lin, C. C. Ma, K. T. Kuo, et al., "Transcription Factor Elf3 Modulates Vasopressin-Induced Aquaporin-2 Gene Expression in Kidney Collecting Duct Cells," *Frontiers in Physiology* 10 (2019): 1308.
17. M. Yasui, S. M. Zelenin, G. Celsi, and A. Aperia, "Adenylate Cyclase-Coupled Vasopressin Receptor Activates AQP2 Promoter via a Dual Effect on CRE and AP1 Elements," *American Journal of Physiology* 272 (1997): F443–F450.
18. W. Lee, P. Mitchell, and R. Tjian, "Purified Transcription Factor AP-1 Interacts With TPA-Inducible Enhancer Elements," *Cell* 49 (1987): 741–752.
19. F. Petrillo, A. Iervolino, T. Angrisano, et al., "Dysregulation of Principal Cell miRNAs Facilitates Epigenetic Regulation of AQP2 and Results in Nephrogenic Diabetes Insipidus," *Journal of the American Society of Nephrology* 32 (2021): 1339–1354.
20. Y. Zheng and D. Pan, "The Hippo Signaling Pathway in Development and Disease," *Developmental Cell* 50 (2019): 264–282.
21. H. S. Choi, H. J. Jang, M. K. Kristensen, and T. H. Kwon, "TAZ Is Involved in Breast Cancer Cell Migration via Regulating Actin Dynamics," *Frontiers in Oncology* 14 (2024): 1376831.
22. J. S. Mo, H. W. Park, and K. L. Guan, "The Hippo Signaling Pathway in Stem Cell Biology and Cancer," *EMBO Reports* 15 (2014): 642–656.
23. Y. Zhang, H. Huang, Y. Kong, et al., "Kidney Tubular Transcription Co-Activator, Yes-Associated Protein 1 (YAP), Controls the Expression of Collecting Duct Aquaporins and Water Homeostasis," *Kidney International* 103 (2023): 501–513.
24. E. J. Lee, E. Seo, J. W. Kim, et al., "TAZ/Wnt-Beta-Catenin/c-MYC Axis Regulates Cystogenesis in Polycystic Kidney Disease," *Proceedings of the National Academy of Sciences of the United States of America* 117 (2020): 29001–29012.
25. S. W. Plouffe, K. C. Lin, J. L. Moore, 3rd, et al., "The Hippo Pathway Effector Proteins YAP and TAZ Have Both Distinct and Overlapping Functions in the Cell," *Journal of Biological Chemistry* 293 (2018): 11230–11240.
26. D. Hilman and U. Gat, "The Evolutionary History of YAP and the Hippo/YAP Pathway," *Molecular Biology and Evolution* 28 (2011): 2403–2417.
27. H. Cho, J. Kim, J. H. Ahn, et al., "YAP and TAZ Negatively Regulate Prox1 During Developmental and Pathologic Lymphangiogenesis," *Circulation Research* 124 (2019): 225–242.
28. J. H. Jun, E. J. Lee, M. Park, J. Y. Ko, and J. H. Park, "Reduced Expression of TAZ Inhibits Primary Cilium Formation in Renal Glomeruli," *Experimental & Molecular Medicine* 54 (2022): 169–179.
29. J. A. Kim, M. J. Kwon, W. Lee-Kwon, S. Y. Choi, S. Sanada, and H. M. Kwon, "Modulation of TonEBP Activity by SUMO Modification in Response to Hypertonicity," *Frontiers in Physiology* 5 (2014): 200.
30. W. Y. Kim, S. A. Nam, A. Choi, et al., "Atg7-Dependent Canonical Autophagy Regulates the Degradation of Aquaporin 2 in Prolonged Hypokalemia," *Scientific Reports* 9 (2019): 3021.
31. H. J. Jang, E. Park, H. J. Jung, and T. H. Kwon, "Poly(ADP-Ribose) Polymerase-1 Affects Vasopressin-Mediated AQP2 Expression in Collecting Duct Cells of the Kidney," *American Journal of Physiology. Renal Physiology* 326 (2024): F69–F85.
32. E. J. Park, J. S. Lim, H. J. Jung, E. Kim, K. H. Han, and T. H. Kwon, "The Role of 70-kDa Heat Shock Protein in dDAVP-Induced AQP2 Trafficking in Kidney Collecting Duct Cells," *American Journal of Physiology. Renal Physiology* 304 (2013): F958–F971.
33. E. J. Park, H. J. Jung, H. J. Choi, J. I. Cho, H. J. Park, and T. H. Kwon, "miR-34c-5p and CaMKII Are Involved in Aldosterone-Induced Fibrosis in Kidney Collecting Duct Cells," *American Journal of Physiology. Renal Physiology* 314 (2018): F329–F342.
34. S. J. Tingskov, H. J. Choi, M. R. Holst, et al., "Vasopressin-Independent Regulation of Aquaporin-2 by Tamoxifen in Kidney Collecting Ducts," *Frontiers in Physiology* 10 (2019): 948.
35. H. J. Park, M. J. Kong, H. J. Jang, et al., "A Nonbiodegradable Scaffold-Free Cell Sheet of Genome-Engineered Mesenchymal Stem Cells Inhibits Development of Acute Kidney Injury," *Kidney International* 99 (2021): 117–133.
36. H. J. Choi, H. J. Jang, E. Park, et al., "Sorting Nexin 27 Regulates the Lysosomal Degradation of Aquaporin-2 Protein in the Kidney Collecting Duct," *Cells* 9 (2020): 1208.
37. D. Kim, J. M. Paggi, C. Park, C. Bennett, and S. L. Salzberg, "Graph-Based Genome Alignment and Genotyping With HISAT2 and HISAT-Genotype," *Nature Biotechnology* 37 (2019): 907–915.
38. M. Pertea, G. M. Pertea, C. M. Antonescu, T. C. Chang, J. T. Mendell, and S. L. Salzberg, "StringTie Enables Improved Reconstruction of a Transcriptome From RNA-Seq Reads," *Nature Biotechnology* 33 (2015): 290–295.
39. Y. Zhou, B. Zhou, L. Pache, et al., "Metascape Provides a Biologist-Oriented Resource for the Analysis of Systems-Level Datasets," *Nature Communications* 10 (2019): 1523.
40. Q. Y. Lei, H. Zhang, B. Zhao, et al., "TAZ Promotes Cell Proliferation and Epithelial-Mesenchymal Transition and Is Inhibited by the Hippo Pathway," *Molecular and Cellular Biology* 28 (2008): 2426–2436.
41. K. Isobe, H. J. Jung, C. R. Yang, et al., "Systems-Level Identification of PKA-Dependent Signaling in Epithelial Cells," *Proceedings of the National Academy of Sciences of the United States of America* 114 (2017): E8875–E8884.
42. L. Xiang, D. M. Gilkes, H. Hu, et al., "HIF-1alpha and TAZ Serve as Reciprocal Co-Activators in Human Breast Cancer Cells," *Oncotarget* 6 (2015): 11768–11778.
43. W. H. Yang, C. C. Ding, T. Sun, et al., "The Hippo Pathway Effector TAZ Regulates Ferroptosis in Renal Cell Carcinoma," *Cell Reports* 28 (2019): 2501–2508.

44. V. Mondal, P. J. Higgins, and R. Samarakoon, "Emerging Role of Hippo-YAP (Yes-Associated Protein)/TAZ (Transcriptional Coactivator With PDZ-Binding Motif) Pathway Dysregulation in Renal Cell Carcinoma Progression," *Cancers* 16 (2024): 2758.
45. E. Enzo, G. Santinon, A. Pocaterra, et al., "Aerobic Glycolysis Tunes YAP/TAZ Transcriptional Activity," *EMBO Journal* 34 (2015): 1349–1370.
46. I. Valencia-Sama, Y. Zhao, D. Lai, H. J. Janse van Rensburg, Y. Hao, and X. Yang, "Hippo Component TAZ Functions as a Co-Repressor and Negatively Regulates DeltaNp63 Transcription Through TEA Domain (TEAD) Transcription Factor," *Journal of Biological Chemistry* 290 (2015): 16906–16917.
47. H. Zhang, C. Y. Liu, Z. Y. Zha, et al., "TEAD Transcription Factors Mediate the Function of TAZ in Cell Growth and Epithelial-Mesenchymal Transition," *Journal of Biological Chemistry* 284 (2009): 13355–13362.
48. M. A. Maxwell and G. E. Muscat, "The NR4A Subgroup: Immediate Early Response Genes With Pleiotropic Physiological Roles," *Nuclear Receptor Signaling* 4 (2006): e002.
49. D. Campos-Melo, D. Galleguillos, N. Sanchez, K. Gysling, and M. E. Andres, "Nur Transcription Factors in Stress and Addiction," *Frontiers in Molecular Neuroscience* 6 (2013): 44.
50. F. Jeanneteau, C. Barrere, M. Vos, et al., "The Stress-Induced Transcription Factor NR4A1 Adjusts Mitochondrial Function and Synapse Number in Prefrontal Cortex," *Journal of Neuroscience* 38 (2018): 1335–1350.
51. Y. Tao, C. Tang, J. Wei, Y. Shan, X. Fang, and Y. Li, "Nr4a1 Promotes Renal Interstitial Fibrosis by Regulating the p38 MAPK Phosphorylation," *Molecular Medicine* 29 (2023): 63.
52. K. Palumbo-Zerr, P. Zerr, A. Distler, et al., "Orphan Nuclear Receptor NR4A1 Regulates Transforming Growth Factor-Beta Signaling and Fibrosis," *Nature Medicine* 21 (2015): 150–158.
53. H. Wang, Z. Wei, C. Xu, et al., "SPDEF Ameliorates UUO-Induced Renal Fibrosis by Transcriptional Activation of NR4A1," *Molecular Medicine* 30 (2024): 282.
54. S. Ma, Z. Meng, R. Chen, and K. L. Guan, "The Hippo Pathway: Biology and Pathophysiology," *Annual Review of Biochemistry* 88 (2019): 577–604.
55. A. Totaro, T. Panciera, and S. Piccolo, "YAP/TAZ Upstream Signals and Downstream Responses," *Nature Cell Biology* 20 (2018): 888–899.
56. Z. Li, Y. Wang, Y. Zhu, et al., "The Hippo Transducer TAZ Promotes Epithelial to Mesenchymal Transition and Cancer Stem Cell Maintenance in Oral Cancer," *Molecular Oncology* 9 (2015): 1091–1105.
57. Y. Wei, V. L. Z. Hui, Y. Chen, R. Han, X. Han, and Y. Guo, "YAP/TAZ: Molecular Pathway and Disease Therapy," *MedComm* 2023, no. 4 (2020): e340.
58. K. Moriyama, A. Horino, K. Kohyama, Y. Nishito, T. Morio, and H. Sakuma, "Oxygen-Glucose Deprivation Increases NR4A1 Expression and Promotes Its Extranuclear Translocation in Mouse Astrocytes," *Brain Sciences* 14 (2024): 244.
59. L. He, L. Yuan, W. Yu, et al., "A Regulation Loop Between YAP and NR4A1 Balances Cell Proliferation and Apoptosis," *Cell Reports* 33 (2020): 108284.

Supporting Information

Additional supporting information can be found online in the Supporting Information section.